Supporting information

QM computations on complete nucleic acids building blocks: Analysis of the Sarcin-Ricin RNA motif using DFT-D3, HF-3c, PM6-D3H and MM approaches.

*Holger Kruse, Marek Havrila, Jiri Sponer**

*Corresponding author: sponer@ncbr.muni.cz

Comparison of backbone angles in key suites 2, 3 and 4: X-ray vs. X-ray structure after optimization.

Table S1 and Table S2 show the backbone angles of both X-ray structures after optimizations at the four levels of theories for the three most important backbone suites (2, 3 and 4). Note that the 1S72 structure is of low resolution (2.4 Å) and thus a qualitative comparison is not advised. For methodological details, see the main manuscript.

Table S1. Backbone and glycosidic torsional angles for the key suites of the QM and MM optimizations of the 1S72 X-ray structure in degrees.

	suite 2					suite 3					suite 4				
	X-ray	QM	GB	PB	APBS	**X-ray**	QM	GB	PB	APBS	**X-ray**	QM	GB	PB	APBS
δ-1	**84**	78	76	77	75	**148**	154	123	133	139	**148**	151	148	150	149
ε-1	**187**	197	194	196	194	**234**	269	271	248	237	**183**	198	191	191	187
ζ-1	**81**	91	89	87	85	**196**	170	186	188	188	**150**	142	147	146	150
α	**325**	308	309	310	321	**287**	267	276	283	292	**291**	288	280	280	280
β	**232**	244	267	266	248	**82**	76	65	75	77	**149**	152	159	162	159
γ	**175**	168	175	168	170	**179**	176	182	179	177	**45**	43	46	46	51
δ	**148**	154	123	133	139	**148**	151	148	150	149	**84**	79	83	90	88
χ-1	**205**	207	218	201	205	**201**	209	190	197	198	**269**	262	270	271	271
χ	**201**	209	190	197	198	**269**	262	270	271	271	**185**	188	186	185	189

Table S2. Backbone and glycosidic torsional angles for the key suites of the QM and MM optimizations of the high-resolution 483D X-ray structure in degrees.

	suite 2					suite 3					suite 4				
angles	**X-ray**	QM	GB	PB	APBS	**X-ray**	QM	GB	PB	APBS	**X-ray**	QM	GB	PB	APBS
δ-1	**81**	82	73	73	78	**151**	147	143	151	150	**147**	149	149	149	145
ε -1	**199**	227	188	196	205	**267**	269	269	268	265	**194**	199	188	195	193
ζ-1	**61**	37	49	52	55	**157**	160	172	161	159	**142**	139	151	144	145
α	**168**	179	157	148	165	**262**	268	274	273	275	**288**	285	279	282	284
β	**142**	136	154	161	148	**93**	85	68	77	81	**151**	149	160	158	157
γ	**48**	57	54	58	53	**178**	173	184	179	178	**42**	46	46	48	48
δ	**151**	147	143	151	150	**147**	149	149	149	145	**90**	81	84	90	87
χ-1	**213**	207	218	216	217	**224**	208	208	227	225	**261**	268	271	265	266
χ	**224**	208	208	227	225	**261**	268	271	265	266	**183**	188	189	187	187

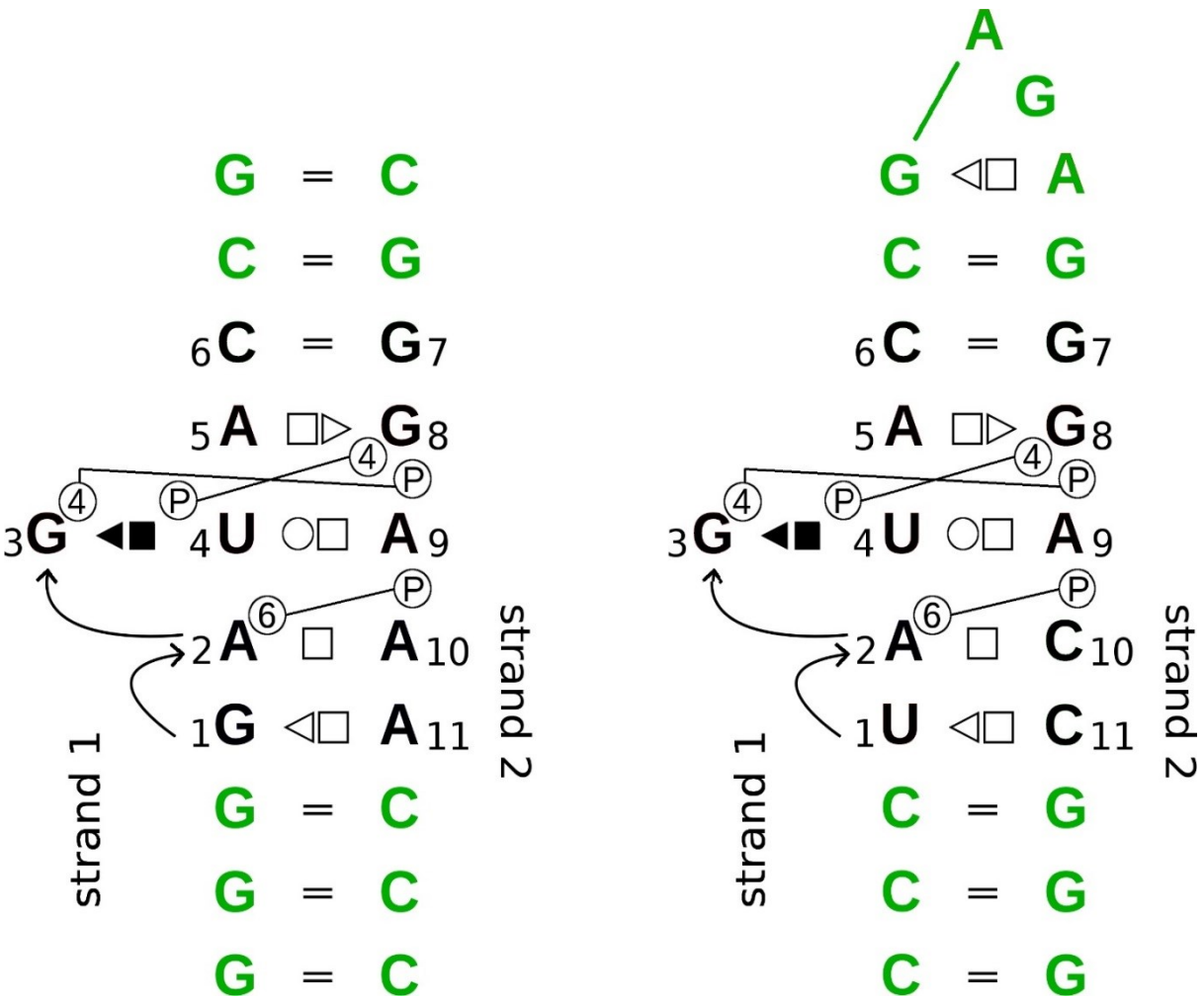

Figure S1. 2D representations of simulated Sarcin-Ricin loops. 1S72 SR loop with GU wobble base pairs replaced by canonical GC base pairs (left) and 483D SR loop with terminal UA base pair replaced by canonical CG base pair (right). Region used for detailed QM and MM study of energetics of different backbone conformations is black. Standard annotations of base pair (bp) (Leontis 2002) and base-phosphate (BPh) (Zirbel 2009) interactions are used.

Extended details on the MD simulations

Files with topology and coordinates were generated by the X-leap module. Using X-leap we added Na^+ ions to neutralize the system and a octahedral box of explicit water solvent with minimal distance of 10 Å between border of box and solute. Established equilibration and production inputs were used. The system was heated, minimized and equilibrated in several steps before the productive MD run. A decreasing force constant was applied to the atoms of the solute during minimization, equilibration and thermalization in order to fix their positions. The last step in the setup was a 50 ps MD run free of constraints. Explicit solvent MD simulations were performed using Particle Mesh Ewald molecular dynamics method. The value of non-bonded cut-off was 9 Å and integration time was 2 fs. SHAKE constraints were applied to all hydrogens to allow longer time step. MD simulations were carried out with constant pressure boundary conditions and constant temperature of 300 K. The Berendsen weak-coupling algorithm was used for temperature regulation.

Table S3. Time windows for structural averaging of the MD trajectory. This Table summarizes exact portions of the trajectories that were used to get the starting structures.

conformation	time window for 1S72 / ns	time window for 483D / ns
equilibrated X-ray[a]	0.0 – 0.05	0.00 – 0.05
2b/3a/4a	4.0 – 4.1	0.71 -0.77
2a/3b/4b	12.4 – 12.5	-
2b/3b/4b	14.6 – 14.7	-
2a/3c/4c	46.5 – 46.6	10.1 – 10.2
2a/3c/4a	57.4 – 57.5	6.7 – 6.8
2a/3c/4d	115.2 – 115.3	-
2b/3c/4c	73.4 – 73.5	-

[a] close to the structure after the initial MD equilibration process. This structure was used in additional computation and is not included in the main Tables (see the main text for further explanations, for the 483D initial structure see also the additional explanation in this Supporting Information file).

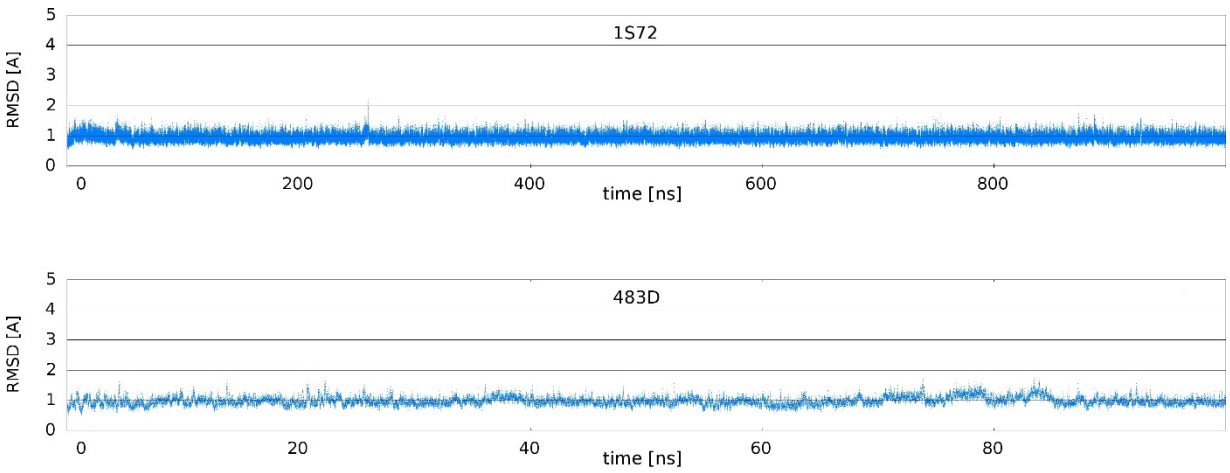

Figure S2. RMSD development of the non-canonical segments (black part in Figure S1) in the MD simulations of 1S72 and 483D SR loops, compared to the X-ray geometry. Note that although the RMSD is low due to the overall stiffness of the SRL, the native backbone conformation is lost in the simulations.

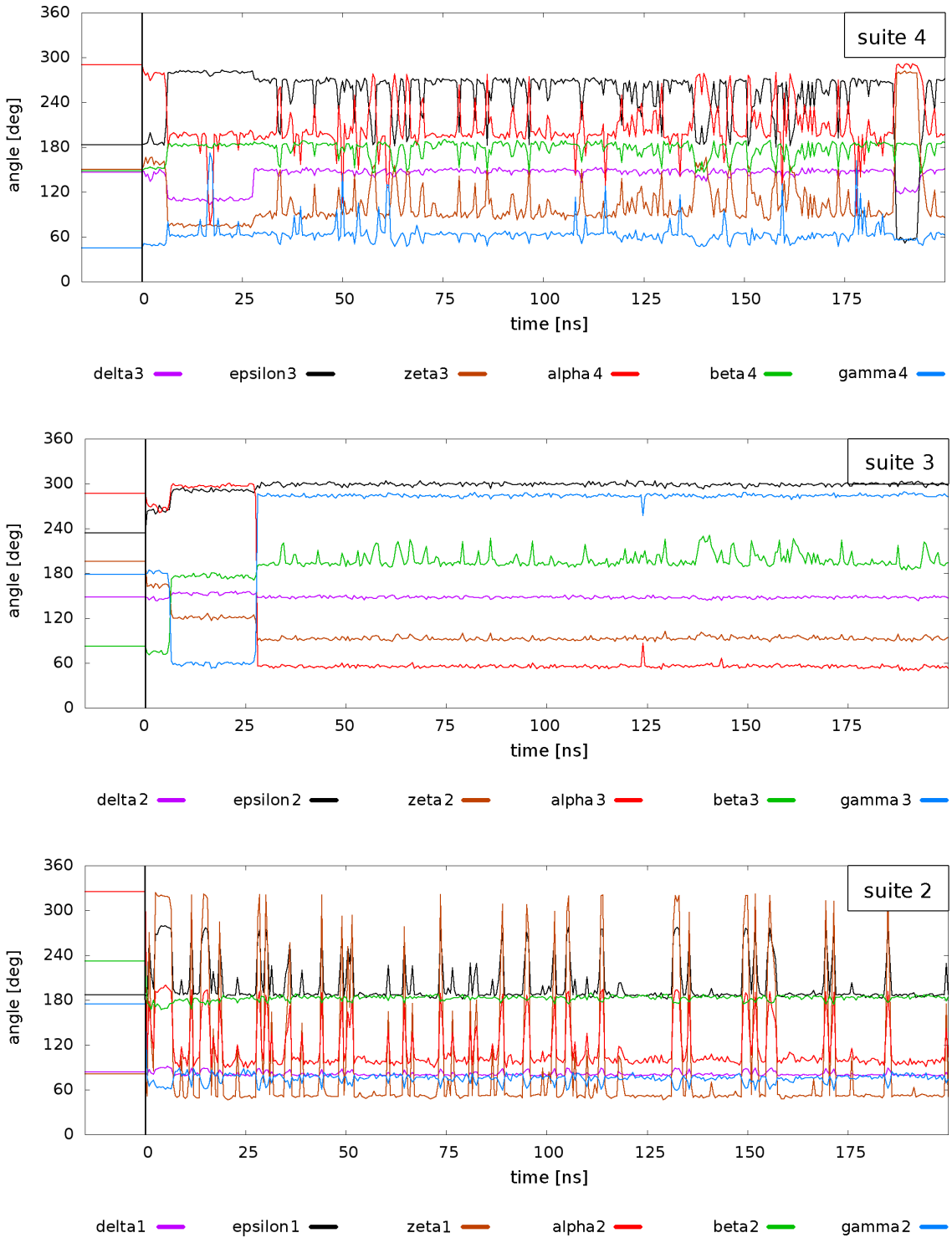

Figure S3. Development of backbone torsion angles of the 1-4 nucleotide segment during the first 200 ns of MD simulation of the 1S72 SR loop. The X-ray values are represented by horizontal lines in the left part of the Figure. Suite 4 is in **#a** geometry at the start of the simulation and then fluctuates between **#a** and **6g** geometries. Suite 3 starts in **4s** geometry that is quickly lost in simulation while initial geometry of suite 2 is not classified. The geometries of suites 2 and 3 observed in simulation do not fit any known suite conformation. Note the loss of low value of β3 which is characteristic for the structure in suite 3. It is caused by force field inaccuracy, as discussed elsewhere (Mladek 2011). Other suites (not shown in the Figure) are, with exception of α-γ flips, very stable and conserve the X-ray geometry.

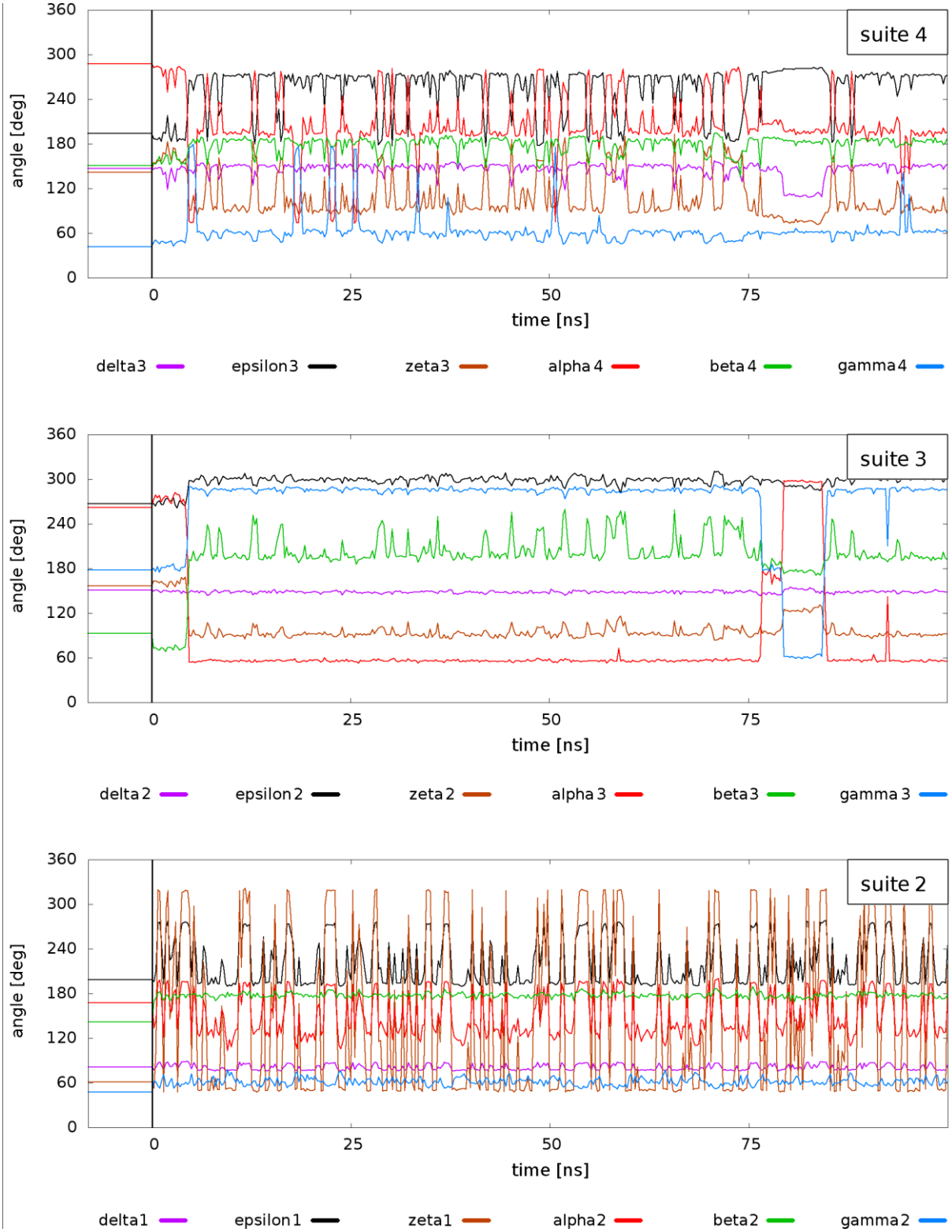

Figure S4. Development of backbone torsion angles of the 1-4 nucleotide segment during the first 200 ns of MD simulation of the 483D SR loop. The X-ray values are represented by horizontal lines in the left part of the Figure.

MM-PBSA free energy along the trajectory

MM-PBSA free energy calculations were done using AmberTools13 applying the mmpbsa.py script. Default values were used except for the grid size, which was set to 0.2 Å (scale=5) and the ionic strength that was set to 0.2 M (istrng=200). Different grid sizes and ionic strengths were tested and did not change the profile significantly.

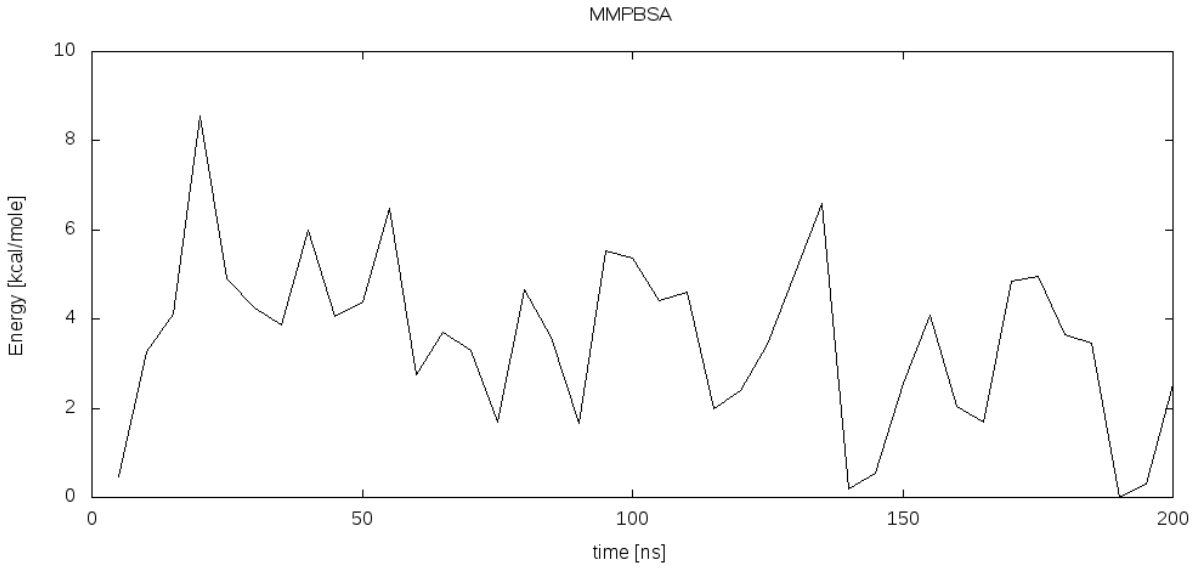

Figure S5. MM-PBSA free energy calculation development along the 1S72 MD trajectory. The first calculated free energy is set to zero and used as the reference point. Each point on the graph corresponds to a 5 ns window and is calculated by averaging energies of 50 snapshots separated by 100 ps steps.

Table S4. 1S72 MD structure backbone families. The *suiteness*, given in brackets (range 0.01 to 1), indicates the agreement of the geometry to the backbone family classification, where 1 shows ideal agreement. If a given suite does not fit to any family no entry is made.

Conformation[a]	suite 2	suite 3	suite 4
X	-	**4s** (0.515)	**#a** (0.939)
2b/3a/4a	-	**4s** (0.748)	**#a** (0.800)
2a/3b/4b	**5p** (0.089)[b]	-	-
2b/3b/4b	-	-	-
2a/3c/4c	**5p** (0.015)[b]	-	**6g** (0.771)
2a/3c/4a	**5p** (0.139)[b]	-	**#a** (0.769)
2a/3c/4d	**5p** (0.138)[b]	-	**6n** (0.559)
2b/3c/4c	-	-	**6g** (0.719)

[a]cf. Table S3 for exact definition of the conformation.

[b] This family is excluded from the consensus cluster list, but may be included in the future. α angle around 100°, between **5p** and **5z**.

Table S5. 483D MD structure backbone families. The suiteness, given in brackets (range 0.01 to 1), indicates the agreement of the geometry to the backbone family classification, where 1 shows ideal agreement. If a given suite does not fit to any family no entry is made.

Conformation[a]	suite 2	suite 3	suite 4
X	**5z** (0.888)	**4s** (0.602)	**#a** (0.923)
2b/3a/4a	-	**4s** (0.727)	**#a** (0.836)
2a/3c/4c	**5z** (0.019)[c]	-	**6g** (0.655)
2a/3c/4a	**5p** (0.025)[b,c]	-	**#a** (0.749)

[a] cf. Table S3 for exact definition of the conformations.

[b] This family is excluded from the consensus cluster list, but may be included in the future.

[c] α angles: *2a/3c/4c* =122°; *2a/3c/4a* =115°. Between **5z** and **5p**.

Comment on the 5z family in the 483D equilibrated structure

For 1S72 simulation no *2a/3a/4a* conformation is available since the MD simulation rapidly changes the initial X-ray geometry and no *2a* substate (or any substate being close to the **5z** family) in suite 2 is sampled while suites 3 and 4 are still within their *3a* and *4a* substates. However, for the 483D structure it is possible to locate a conformation of suite 2 still being in the native **5z** family within the first 400ps of the simulation. This conformation is denoted *2a'* to differentiate it to *2a*, which has an extremely low suiteness for the **5z** family (cf. Table S5). This leads to a *2a'/3a/4a* overall conformation and can be considered as the native conformation. We averaged snapshots in the time window of 0 to 50ps after the simulation start to generate a conformation close to the equilibrated X-ray structure from which the MD simulation started for 483D with suite 2 having **5z** conformation. This conformations was then optimized with MM-GB and subsequently a single-point calculation using QM (COSMO-TPSS-D3/def2-TZVP) was performed. This 'early MD' structure, which essentially corresponds to the native structure, is at the QM level (QM//GB) by 4.9 kcal/mol more stable than our selected reference *2b/3a/4a* conformation. Also its MM level (GB//GB) energy is rather similar, being 8.9 kcal/mol more stable than the *2b/3a/4a* conformation. We did not use this number in the main text Tables to keep the paper simple, because the main text analysis is based primarily on the 1S72 simulation structures not sampling the *2a'/3a/4a* conformation and the 438D computations were done later for verification purposes.

QM optimization of the 483D conformations

The QM optimizations lead to even larger geometrical changes than for the 1S72 conformations, making a comparison with the 1S72 QM optimizations difficult. The changes again include formation of the G8/U4 BPh interaction in the *2a*/*3c*/*4c* QM optimization with the *4c* → *4a* rearrangement. We also observe formation of non-native BPh interactions affecting the base pairing of the U1-C11 and A2-C10 base pairs. However, an additional major structural change is the loss of base pairing for the lower two base pairs (U1-C11, A2-C10) in the QM optimization for the *2a*/*3c*/*4c* and *2a*/*3c*/*4a* conformations. The effects are more pronounced in 483D than in 1S72 SRL since the base pairing of the 'flexible' region of 483D is considered weaker than in 1S72, because of the different nucleobases involved.[1] These rearrangements are affecting each conformation to a different extent, impeding

comparisons of energies. Note that the 483D SRL has intrinsically weaker pairing than 1S72 SRL in this region.[2]

For the *2a*/*3c*/*4c* conformation, we see again the 5'-end hydroxyl H-bond in the QM optimized structures but it does not form in the other structures. Thus, while in Table 1 we added an energy correction (data in parentheses) to structures lacking these terminal H-bonds, in Table 2 we added a correction with the opposite sign to the energy of *2a*/*3c*/*4c*. The correction is again estimated from the difference between the terminal dinucleotide assuming geometries seen in the *2a*/*3c*/*4c* and *2a*/*3c*/*4a* optimized structures, as described above. Due to the large differences between the lower two base pairs the QM-optimized *2a*/*3c*/*4c* and *2a*/*3c*/*4a* conformations, although having after rearrangement very similar suites 2, 3 and 4, have very different energies.

Additional geometry analyses data

Table S6. Survey of changes of the backbone and glycosidic torsional angles for the optimized structures across all substates listed in the Table 3 (1S72 + water) covering all occurrences of the listed angles. The changes are calculated against the X-ray structure for state X and against the respective MD-based starting structures for all the other states (angle(initial) – angle(optimized). Range(+) and range(-) show the maximal deviations; negative deviations mean the angle becomes larger; MAD is the mean absolute deviation (MAD). This Table is equivalent to Table 4 in the main MS which shows the same data but for structures without the water molecules. The data shows only slightly larger deviations than the corresponding data for the 1S72 conformations without the explicit water (Table 4, main manuscript).

	MM GB			MM PB			MM APBS			QM COSMO		
	range(+)	range(-)	MAD	range(+)	range(-)	MAD	range(+)	range(-)	MAD	range(+)	range(-)	MAD
α	15.9	−19.1	4.2	12.5	−17.3	2.8	4.6	−12.4	1.6	81.6	−21.9	8.6
β	35.6	−17.0	4.5	33.5	−8.6	3.3	15.6	−5.8	1.6	63.7	−48.6	14.4
γ	18.5	−11.9	3.6	14.8	−11.3	2.6	9.3	−5.6	1.4	13.7	−27.8	5.6
δ	11.8	−23.5	3.0	6.4	−15.7	1.8	8.0	−9.2	1.4	12.5	−15.4	3.5
ε	37.6	−13.3	4.5	19.0	−15.5	3.0	6.4	−7.7	1.6	53.0	−73.8	12.4
ζ	13.7	−22.4	4.0	15.3	−17.2	3.1	13.6	−7.4	1.5	52.7	−68.5	12.4
χ	16.4	−14.8	4.6	7.8	−6.8	1.4	4.6	−3.0	1.0	30.7	−39.3	11.5

Overview of structural key features

The following Tables give a short – and thus incomplete – overview of structural features that we consider as key components in the discussion about energetical differences.

Table S7. Key structural features of the conformations derived from the S172 structure, its simulation and subsequent optimizations. Cf. Table 1 in the main text.

conformation	initial & optimized structures	RMSD to initial structure /Å	5'-OH rotation	native 4-8 BPh int.	non-native BPh interaction distances[1]			RMSD to QM conformation *2a/3c/4a* in Å
					5-6 / Å	1-11 / Å	1-10 / Å	
X	X-ray	0.00	no	yes	4.24	4.18	3.98	-
	GB	0.67	no	yes	2.92	3.50	3.36	-
	PB	0.29	no	yes	4.66	4.74	4.22	-
	APBS	0.27	no	yes	4.57	4.48	4.36	-
	QM	1.25	no	yes	1.84	2.01	3.85	0.83
2b/3a/4a	MD	0.00	no	yes	3.97	4.03	3.23	-
	GB	0.47	no	yes	1.94	4.18	1.90	-
	PB	0.10	no	yes	4.14	4.10	3.20	-
	APBS	0.07	no	yes	3.98	4.00	3.23	-
	QM	0.90	yes	yes	1.89	2.06	2.06	0.75
2a/3b/4b	MD	0.00	no	no	5.51	4.00	3.49	-
	GB	0.55	no	no	3.74	4.58	3.80	-
	PB	0.17	no	no	5.63	4.53	3.59	-
	APBS	0.09	no	no	5.56	4.0	3.50	-
	QM	1.26	yes	yes	1.86	3.27	2.50	0.60
2b/3b/4b	MD	0.00	no	no	4.5	4.47	3.91	-
	GB	0.48	no	no	3.33	4.14	1.94	-
	PB	0.10	no	no	4.57	4.43	3.88	-
	APBS	0.07	no	no	4.52	4.44	3.86	-
	QM	0.95	yes	yes	1.86	2.16	1.89	0.80
2a/3c/4c	MD	0.00	no	no	4.17	4.45	3.66	-
	GB	0.50	no	no	2.67	4.43	3.66	-
	PB	0.11	no	no	4.24	4.42	4.51	-
	APBS	0.07	no	no	4.14	4.43	3.64	-
	QM	1.13	yes	yes	1.85	2.22	2.27	0.38
2a/3c/4a	MD	0.00	no	yes	3.91	4.36	3.76	-
	GB	0.49	no	yes	1.90	4.50	3.67	-
	PB	0.10	no	yes	4.12	4.50	3.71	-
	APBS	0.07	no	yes	3.92	4.35	3.74	-
	QM	1.00	no	yes	1.86	2.30	2.13	0.00
2a/3c/4d	MD	0.00	no	no	3.79	4.43	3.90	-
	GB	0.48	no	no	1.91	4.62	3.75	-
	PB	0.09	no	no	3.82	4.54	3.80	-
	APBS	0.07	no	no	3.78	4.41	3.85	-
	QM	1.13	yes	yes	1.87	2.14	2.62	0.49
2b/3c/4c	MD	0.00	no	no	4.09	4.10	3.26	-
	GB	0.43	no	no	3.32	4.13	1.93	-
	PB	0.08	no	No	4.14	4.15	3.20	-

	APBS	0.07	no	No	4.08	4.08	3.23		-
	QM	1.18	yes	Yes	1.84	2.38	2.10		0.49

[1] 5-6 - A5(O2P)/C6(H42); 1-11 - G1(H21)/A11(O2P); 1-10 - G1(H1)/A10(O2P)

Table S8. Key structural features of the conformations of the structure 1S72. Inclusion of one explicit water molecule. Cf. Table 3 in the main text.

conformation	initial & optimized structures	RMSD to initial structure /Å	5'-OH rotation	native 4-8 BPh int.	non-native BPh interactions[1]			BPh interaction and explicit water[2]		RMSD to QM conformation *2a/3c/4a* in Å
					5-6 / Å	1-11 / Å	1-10 / Å	4-8	5-6	
X	X-ray	0.00	x	yes	4.24	4.18	3.98			-
	GB	0.67	x	yes	2.92	3.50	3.36			-
	PB	0.29	x	yes	4.66	4.74	4.22			-
	APBS	0.27	x	yes	4.57	4.48	4.36			-
	QM	1.25	x	yes	1.84	2.01	3.85	0	s	
2b/3a/4a	MD	0.00	x	yes	3.97	4.03	3.23			-
	GB	0.47	x	yes	1.94	4.18	1.90			-
	PB	0.10	x	yes	4.14	4.10	3.20			-
	APBS	0.07	x	yes	3.98	4.00	3.23			-
	QM	0.90	yes	yes	1.89	2.06	2.06	0	s	
2a/3b/4b	MD	0.00	x	x	5.51	4.00	3.49			-
	GB	0.55	x	x	3.74	4.58	3.80			-
	PB	0.17	x	x	5.63	4.53	3.59			-
	APBS	0.09	x	x	5.56	4.00	3.50			-
	QM	1.26	yes	yes	1.86	3.27	2.50	s	s	
2b/3b/4b	MD	0.00	x	x	4.50	4.47	3.91			-
	GB	0.48	x	x	3.33	4.14	1.94			-
	PB	0.10	x	x	4.57	4.43	3.88			-
	APBS	0.07	x	x	4.52	4.44	3.86			-
	QM	0.95	yes	yes	1.86	2.16	1.89	s	n	
2a/3c/4c	MD	0	x	x	4.17	4.45	3.66			-
	GB	0.50	x	x	2.67	4.43	3.66			-
	PB	0.11	x	x	4.24	4.42	4.51			-
	APBS	0.07	x	x	4.14	4.43	3.64			-
	QM	1.13	yes	yes	1.85	2.22	2.27	n	s	0.40
2a/3c/4a	MD	0.00	x	yes	3.91	4.36	3.76			-
	GB	0.49	x	yes	1.90	4.50	3.67			-
	PB	0.10	x	yes	4.12	4.50	3.71			-
	APBS	0.07	x	yes	3.92	4.35	3.74			-
	QM	1.00	x	yes	1.86	2.30	2.13	0	s	0.00
2a/3c/4d	MD	0.00	x	x	3.79	4.43	3.90			-
	GB	0.48	x	x	1.91	4.62	3.75			-
	PB	0.09	x	x	3.82	4.54	3.80			-
	APBS	0.07	x	x	3.78	4.41	3.85			-
	QM	1.13	yes	yes	1.87	2.14	2.62	s	n	
2b/3c/4c	MD	0.00	x	x	4.09	4.10	3.26			-

	GB	0.43	x	x	3.32	4.13	1.93			-
	PB	0.08	x	x	4.14	4.15	3.20			-
	APBS	0.07	x	x	4.08	4.08	3.23			-
	QM	1.18	yes	yes	1.84	2.38	2.10	s	n	

[1] 5-6 - A5(O2P)/C6(H42); 1-11 - G1(H21)/A11(O2P); 1-10 - G1(H1)/A10(O2P)

[2] behaviour of the explicit water molecule regarding the respective BPh interaction: s = stabilizing/bridging; n= not stabilizing/bridging; 0 = no interference, direct BPh interaction present in initial structure.

Table S9. Key structural features of the conformations based on the high-resolution structure 483D and its simulation. Cf. Table 2 in the main text.

conformation	initial & optimized structures	RMSD to initial structure / Å	5'-OH rotation	native 4-8 BPh int.	non-native BPh interaction distances[1]			RMSD to QM conformation *2a/3c/4a* in Å
					5-6 / Å	1-11 / Å	1-10 / Å	
X	X-ray	0.00	no	yes	4.21	4.18	3.86	-
	GB	0.63	no	yes	3.04	2.13	3.86	-
	PB	0.22	no	yes	4.72	4.40	4.05	-
	APBS	0.19	no	yes	4.47	4.37	4.06	-
	QM	0.96	no	yes	1.86	1.91	3.59	0.80
2b/3a/4a	MD	0.00	no	yes	4.01	3.73	4.23	-
	GB	0.53	no	yes	1.92	1.89	3.69	-
	PB	0.10	no	yes	4.24	3.46	4.15	-
	APBS	0.07	no	yes	4.02	3.66	4.20	-
	QM	0.83	yes	yes	1.88	2.01	1.90	1.11
2a/3c/4c	MD	0.00	no	no	4.01	3.86	4.74	-
	GB	0.48	no	no	3.45	2.59	4.22	-
	PB	0.11	no	no	4.08	3.76	4.70	-
	APBS	0.07	no	no	3.99	3.82	4.71	-
	QM	1.26	yes	yes	1.89	1.91	4.64	0.48
2a/3c/4a	MD	0.00	no	yes	3.65	3.61	4.32	-
	GB	0.59	no	yes	1.90	1.87	3.97	-
	PB	0.10	no	yes	3.72	3.51	4.28	-
	APBS	0.08	no	yes	3.63	3.57	4.29	-
	QM	0.97	no	yes	1.85	1.94	3.82	0.00

[1] 5-6 - A5(O2P)/C6(H42); 1-10 - U1(H3)/C10(O2P); 10-11 - C10(O2P)/C11(H42)

G8/U4 - BPh interactions

The Table S10 and Table S11 show instances of the U4/G8 base-phosphate (BPh) interaction in the respective conformations for the 1S72 system.

Table S10. BPh interaction length between O2(P) suite 4 to N2(G) suite 8 in Å for the 1S72 structure.

	X-ray/MD	GB_{opt}	PB_{opt}	$APBS_{opt}$	QM_{opt}
X	3.1	2.9	3.0	3.1	2.9
2b/3a/4a	3.3	3.4	3.1	3.3	2.9
2a/3b/4b	6.5	6.0	6.6	6.5	2.9
2b/3b/4b	6.1	5.9	6.2	6.2	2.9
2a/3c/4c	5.8	5.8	5.9	5.8	3.1
2a/3c/4a	3.7	3.5	3.6	3.7	3.1
2a/3c/4d	6.9	6.5	6.8	7.0	3.4
2b/3c/4c	5.9	5.8	6.0	6.0	3.1

Table S11. BPh interaction length between O2(P) suite 4 to N2(G) suite 8 in Å for the 1S72 structure with inclusion of explicit water.

	X-ray/MD	GB	PB	APBS	QM
X	3.1	2.8	2.9	3.1	2.9
2b/3a/4a	3.3	3.0	3.4	3.4	2.9
2a/3b/4b	6.5	6.4	6.5	6.6	4.8
2b/3b/4b	6.6	5.3	6.4	6.7	5.2
2a/3c/4c	5.8	5.5	5.4	5.9	3.1
2a/3c/4a	3.7	3.6	3.7	3.7	3.0
2a/3c/4d	6.9	6.9	6.9	6.6	5.3
2b/3c/4c	5.9	5.4	5.6	6.0	5.1

Numerical values for the benchmark study

Table S12. Numerical values (kcal/mol) corresponding to the Figure 6 in the main text.

	GB-MM	TPSS-D3	PW6B95-D3	M06-2X	TPSS-gCP-D3	PM6-D3H	HF-3c
X	19.4	23.7	24.5	24.8	24.1	52.7	40.4
2b/3a/4a	0.0	0.0	0.0	0.0	0.0	0.0	0.0
2a/3b/4b	3.9	20.3	21.4	23.5	19.8	33.7	38.6
2b/3b/4b	4.1	19.4	18.9	20.3	20.1	24.0	34.5
2a/3c/4c	1.9	14.7	16.0	18.3	13.2	25.9	32.9
2a/3c/4a	-0.1	-4.6	-3.1	-2.4	-6.0	0.6	0.0
2a/3c/4d	1.7	4.0	5.1	6.7	2.7	11.3	15.7
2b/3c/4c	4.1	19.7	20.1	21.4	19.8	23.7	35.6

Amber input (minimal, without optimization settings)

MM-GB:

```
&cntrl
nstlim  =0, ntx=1, igb=1, ntf=1, ntc=1, ntb=0, irest=0
/
&end
```

MM-PB:

```
&cntrl
nstlim  =0, ntx=1, ipb=2, ntf=1, ntc=1, ntb=0, irest=0
/
&pb
radiopt=1,space=0.2,dbfopt=1,arcres=0.0625,sprob=1.6
/
&end
```

MM-APBS:

```
&cntrl
  ntx=1, irest=0,  imin=1, maxcyc=0,
  ntpr=1,ntwr=100000,   igb=6, ntb=0, cut = 999.0,
  ntc=1, ntf=1, tol=0.000001,  ntt=0, temp0=300
 &end
 &apbs
   nonlin=0,
   apbs_debug=0,
   apbs_print=0,
   grid=0.15, 0.15, 0.15,
   calc_type=0,
   cmeth=1,
   bcfl=2,
   srfm=1,
   chgm=1,
   pdie=1.0,
   sdie=80.0,
   srad = 1.4,
   radiopt=0,
   calcenergy=1, calcforce=0, calcnpenergy=1, calcnpforce=0,
&end
```

Structures

see provided zip file for structural data

References

1. (a) Correll, C. C.; Wool, I. G.; Munishkin, A., The two faces of the Escherichia coli 23 S rRNA sarcin/ricin domain: the structure at 1.11 A resolution. *J. Mol. Biol.* **1999,** *292* (2), 275-287; (b) Sponer, J.; Jurecka, P.; Hobza, P., Accurate interaction energies of hydrogen-bonded nucleic acid base pairs. *J. Am. Chem. Soc.* **2004,** *126* (32), 10142-10151.

2. Havrila, M.; Réblová, K.; Zirbel, C. L.; Leontis, N. B.; Šponer, J., Isosteric and Nonisosteric Base Pairs in RNA Motifs: Molecular Dynamics and Bioinformatics Study of the Sarcin–Ricin Internal Loop. *J. Phys. Chem. B* **2013,** *117* (46), 14302-14319.